Effects of the laser parameters on the determination of the Sn isotope ratio

Shuichi Hasegawa and Atsuyuki Suzuki
Department of Quantum Engineering and Systems Science, The University of Tokyo, Hongo 7-3-1, Bunkyo-ku, Tokyo 113, Japan
(Received 8 March 1993)

The effects of laser parameters such as intensity, wavelength, and bandwidth on the determination of the Sn isotope ratio are analyzed numerically with density-matrix equations. The bandwidth of the laser is taken into account by the chaotic-field model. We consider the isotopes of Sn that consist of the even-mass isotopes with no nuclear spin and the odd-mass isotopes with a nuclear spin of $\hbar/2$. In the scheme in which a first laser excites atoms to an intermediate state and a second laser ionizes them, the exciting-laser intensity has greater influence on the isotope ratio than the ionizing-laser intensity regardless of the laser bandwidth. As regards the laser bandwidth, a comparison is made between the broad bandwidth that overlaps all intermediate levels of the isotopes and the narrow bandwidth that is small enough to excite only the intermediate level of the even-mass isotopes. The even-mass isotopes whose intermediate level is on resonance are more ionized than the odd-mass isotopes when the intensity of the broadband exciting laser is small, while the odd-mass isotopes are more ionized when the intensity of the narrow-band exciting laser is large. The isotope ratio is sensitive to the exciting-laser wavelength even when the laser bandwidth is broad.

PACS number(s): 32.80.Rm, 42.50.Lc

I. INTRODUCTION

Resonance-ionization mass spectrometry (RIMS) has many applications, such as spectroscopy of high-lying Rydberg states, isotope separation, analysis of trace elements, and determination of isotope ratio [1–6]. RIMS has a great advantage in removing isobaric interferences, because atoms can be element- or isotope- selectively ionized and only desirable elements or isotopes of interest can be introduced into a mass analyzer.

On the other hand, to determine the isotope ratio of trace elements with RIMS, all isotopes need to be ionized to the same degree; it has been shown experimentally [7] and theoretically [8,9] that the ionization of each isotope is dependent on laser-atom parameters even when the laser bandwidth is large enough to overlap all hyperfine splittings and isotope shifts. In fact, Refs. [8,9] point out that the isotope ratio is dependent on the laser intensity, while all hyperfine levels are excited by a broadband laser. They showed the dependency of the fractional ratio $\beta=(P'-P)/0.5(P'+P)$ on the laser intensity, where P and P' stand for isotope probabilities of even- and odd-mass isotopes, respectively, for the cases of the single-laser scheme [8] and the doubly resonant ionization scheme [9].

Other than laser intensity, bandwidth and detuning should also affect the fractional ratio. We have experimentally investigated influences of other laser parameters on the determination of isotopic abundances of ytterbium [10]. Reference [10] suggests that laser-beam polarizations and applied electric fields also have effects on the fractional ratio on the condition of a simple ionization scheme such as $J=0\rightarrow J'=I\rightarrow$ continuum.

In this paper, we attempt to incorporate the laser parameters which have been found to be influential in the determination of P. In previous studies [8,9], effects of laser bandwidth are taken into account by applying the phase-diffusion model. We employ the chaotic-field model since it is suitable for pulsed-dye lasers [11]. The comparison between two models has been made in many papers [12–14]. They show that the chaotic-field model is less effective than the phase-diffusion model in saturating a single- or multiphoton transition.

Effects of laser line shape are also important, especially for a far-off-resonance region [15–17] because the far wing of a Lorentzian line shape falls off very slowly while a realistic laser line shape resembles a Gaussian which drops much faster than a Lorentzian. However, we calculate the ionization probability of the even- and odd-mass isotopes using the chaotic-field model with the Lorentzian line shape for simplicity of calculation.

II. THEORY

We consider as an example Sn, whose atomic parameters are calculated in Ref. [8]. The energy diagram of Sn is shown in Fig. 1. The ground state of Sn is $|0\rangle=5p^2\,{}^3P_0$. The even-mass isotopes of Sn ($I=0$) have an intermediate level of value 34 914 cm^{-1}, whose configuration is $|1\rangle=5p6s\,{}^3P_1^o$. Because of the nuclear spin ($I=\frac{1}{2}$), the odd-mass isotopes of Sn are split into two hyperfine levels. The energy difference of the two hyperfine levels is 0.26 cm^{-1}. In $|IJFM_F\rangle$ representation, the configuration of the ground state is $|\frac{1}{2}\,0\,\frac{1}{2}\,\frac{1}{2}\rangle$, and those of the intermediate states are $|1'\rangle=|\frac{1}{2}\,1\frac{1}{2}\,\frac{1}{2}\rangle$ and $|2'\rangle=|\frac{1}{2}\,1\frac{3}{2}\,\frac{1}{2}\rangle$, respectively.

The atoms are assumed to be irradiated simultaneously by two independent lasers for exciting and ionizing the atoms. The exciting laser is tuned to the resonance frequency of the even-mass isotopes. To take into account the bandwidth of a laser, we assume that both laser fields are described as chaotic fields whose characteristics are in detail written in [18,19].

Applying the rotating-wave approximation to Bloch equations of the system, we obtain the following density-matrix equations [19,20]:

$$\frac{d}{dt}\sigma_{00}^{nm}=-(2nb_a+2mb_b)\sigma_{00}^{nm}+\frac{1}{\tau_i}\sigma_{11}^{nm}+i\frac{\Omega_{01}}{2}(\sqrt{n+1}\sigma_{10}^{nm}-\sqrt{n}\,\sigma_{10}^{n-1m})-i\frac{\Omega_{10}}{2}(\sqrt{n+1}\sigma_{01}^{nm}-\sqrt{n}\,\sigma_{01}^{n-1m}) , \tag{1}$$

$$\frac{d}{dt}\sigma_{11}^{nm}=-\left[\frac{1}{\tau_1}+2nb_a+2mb_b\right]\sigma_{11}^{nm}-\Gamma\{-(m+1)\sigma_{11}^{nm+1}+(2m+1)\sigma_{11}^{nm}-m\sigma_{11}^{nm-1}\}$$
$$-i\frac{\Omega_{01}}{2}(\sqrt{n+1}\sigma_{10}^{nm}-\sqrt{n}\,\sigma_{10}^{n-1m})+i\frac{\Omega_{10}}{2}(\sqrt{n+1}\sigma_{01}^{nm}-\sqrt{n}\,\sigma_{01}^{n-1m}) , \tag{2}$$

$$\frac{d}{dt}\sigma_{10}^{nm}=\left[i\Delta_1-\left[\frac{1}{2\tau_1}+b_a(2n+1)+2mb_b\right]\right]\sigma_{10}^{nm}-\frac{\Gamma}{2}\{-(m+1)\sigma_{10}^{nm+1}+(2m+1)\sigma_{10}^{nm}-m\sigma_{10}^{nm-1}\}$$
$$-i\frac{\Omega_{10}}{2}\sqrt{n+1}(\sigma_{11}^{nm}-\sigma_{11}^{n+1m})+i\frac{\Omega_{10}}{2}\sqrt{n+1}(\sigma_{00}^{nm}-\sigma_{00}^{n+1m}) , \tag{3}$$

$$\frac{d}{dt}\sigma_{00}^{nm}=-(2nb_a+2mb_b)\sigma_{00}^{nm}+\frac{1}{\tau_{1'}}\sigma_{1'1'}^{nm}+\frac{1}{\tau_{2'}}\sigma_{2'2'}^{nm}+i\frac{\Omega_{01'}}{2}(\sqrt{n+1}\sigma_{1'0}^{nm}-\sqrt{n}\,\sigma_{1'0}^{n-1m})$$
$$-i\frac{\Omega_{1'0}}{2}(\sqrt{n+1}\sigma_{01'}^{nm}-\sqrt{n}\,\sigma_{01'}^{n-1m})+i\frac{\Omega_{02'}}{2}(\sqrt{n+1}\sigma_{2'0}^{nm}-\sqrt{n}\,\sigma_{2'0}^{n-1m})-i\frac{\Omega_{2'0}}{2}(\sqrt{n+1}\sigma_{02'}^{nm}-\sqrt{n}\,\sigma_{02'}^{n-1m}) , \tag{4}$$

$$\frac{d}{dt}\sigma_{1'1'}^{nm}=-\left[\frac{1}{\tau_{1'}}+2nb_a+2mb_b\right]\sigma_{1'1'}^{nm}-\Gamma_{1'}\{-(m+1)\sigma_{1'1'}^{nm+1}+(2m+1)\sigma_{1'1'}^{nm}-m\sigma_{1'1'}^{nm-1}\}$$
$$-i\frac{\Omega_{01'}}{2}(\sqrt{n+1}\sigma_{1'0}^{nm}-\sqrt{n}\,\sigma_{1'0}^{n-1m})+i\frac{\Omega_{1'0}}{2}(\sqrt{n+1}\sigma_{01'}^{nm}-\sqrt{n}\,\sigma_{01'}^{n-1m}) , \tag{5}$$

$$\frac{d}{dt}\sigma_{2'2'}^{nm}=-\left[\frac{1}{\tau_{2'}}+2nb_a+2mb_b\right]\sigma_{2'2'}^{nm}-\Gamma_{2'}\{-(m+1)\sigma_{2'2'}^{nm+1}+(2m+1)\sigma_{2'2'}^{nm}-m\sigma_{2'2'}^{nm-1}\}$$
$$-i\frac{\Omega_{02'}}{2}(\sqrt{n+1}\sigma_{2'0}^{nm}-\sqrt{n}\,\sigma_{2'0}^{n-1m})+i\frac{\Omega_{2'0}}{2}(\sqrt{n+1}\sigma_{02'}^{nm}-\sqrt{n}\,\sigma_{02'}^{n-1m}) , \tag{6}$$

$$\frac{d}{dt}\sigma_{1'0}^{nm}=\left[i\Delta_{1'}-\left[\frac{1}{2\tau_{1'}}+(2n+1)b_a+2mb_b\right]\right]\sigma_{1'0}^{nm}-\frac{\Gamma_{1'}}{2}\{-(m+1)\sigma_{1'0}^{nm+1}+(2m+1)\sigma_{1'0}^{nm}-m\sigma_{1'1'}^{nm-1}\}$$
$$-i\frac{\Omega_{1'0}}{2}\sqrt{n+1}(\sigma_{1'1'}^{nm}-\sigma_{1'1'}^{n+1m})+i\frac{\Omega_{1'0}}{2}\sqrt{n+1}(\sigma_{00}^{nm}-\sigma_{00}^{n+1m})-i\frac{\Omega_{2'0}}{2}(\sqrt{n+1}\sigma_{1'2'}^{nm}-\sqrt{n}\,\sigma_{1'2'}^{n-1m}) , \tag{7}$$

$$\frac{d}{dt}\sigma_{2'0}^{nm}=\left[i\Delta_{2'}-\left[\frac{1}{2\tau_{2'}}+(2n+1)b_a+2mb_b\right]\right]\sigma_{2'0}^{nm}-\frac{\Gamma_{2'}}{2}\{-(m+1)\sigma_{2'0}^{nm+1}+(2m+1)\sigma_{2'0}^{nm}-m\sigma_{2'0}^{nm}\}$$
$$-i\frac{\Omega_{2'0}}{2}\sqrt{n+1}(\sigma_{2'2'}^{nm}-\sigma_{2'2'}^{n+1m})+i\frac{\Omega_{2'0}}{2}\sqrt{n+1}(\sigma_{00}^{nm}-\sigma_{00}^{n+1m})-i\frac{\Omega_{1'0}}{2}(\sqrt{n+1}\sigma_{2'1'}^{nm}-\sqrt{n}\,\sigma_{2'1'}^{n-1m}) , \tag{8}$$

$$\frac{d}{dt}\sigma_{1'2'}^{nm}=\left\{-i\omega_{1'2'}-\left[\frac{1}{2}\left[\frac{1}{\tau_{1'}}+\frac{1}{\tau_{2'}}\right]+2nb_a+2nm_b\right]\right\}\sigma_{1'2'}^{nm}-\frac{\Gamma_{1'}+\Gamma_{2'}}{2}\{-(m+1)\sigma_{1'2'}^{nm+1}+(2m+1)\sigma_{1'2'}^{nm}-m\sigma_{1'2'}^{nm-1}\}$$
$$+i\frac{\Omega_{1'0}}{2}(\sqrt{n+1}\sigma_{02'}^{nm}-\sqrt{n}\,\sigma_{02'}^{n-1m})-i\frac{\Omega_{02'}}{2}(\sqrt{n+1}\sigma_{1'0}^{nm}-\sqrt{n}\,\sigma_{1'0}^{n-1m}) , \tag{9}$$

with $n,m=0,1,2,\ldots$ denoting the correlation order of each laser. The Rabi frequencies which appear in the above equations are defined as follows:

$$\Omega_{ij}=2\hbar^{-1}\mu_{ij}\langle|\epsilon|^2\rangle^{1/2} . \tag{10}$$

The population of each level is given by

$$\langle\sigma_{nn}\rangle=\sigma_{nn}^{00} . \tag{11}$$

The ionization probability of the even-mass isotopes is defined as

$$P(t)=1-\sigma_{00}^{00}-\sigma_{11}^{00} . \tag{12}$$

That of the odd-mass isotopes is also defined as

$$P'(t)=1-\sigma_{00}^{00}-\sigma_{1'1'}^{00}-\sigma_{2'2'}^{00} . \tag{13}$$

The atomic parameters of Sn that we will use in the fol-

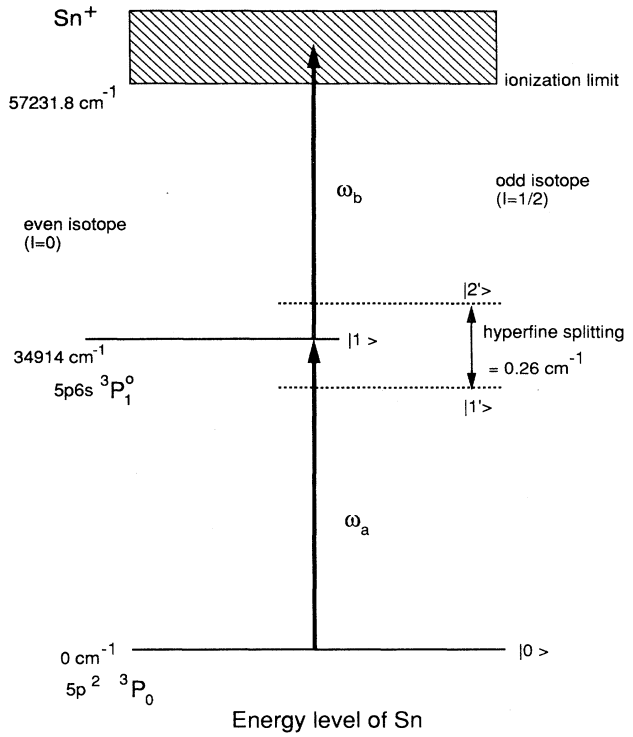

FIG. 1. Resonance-ionization scheme of Sn calculated in this study.

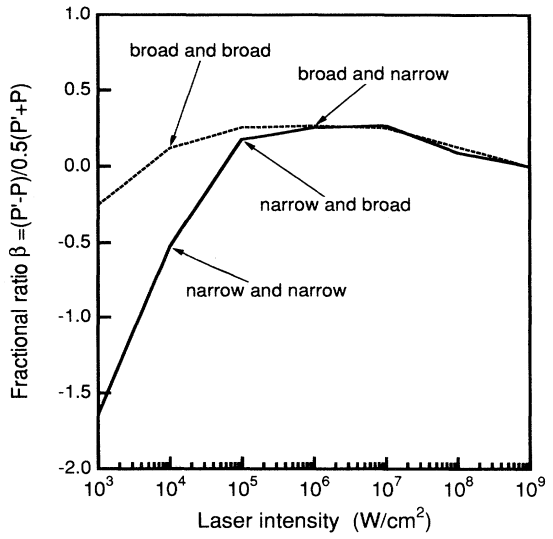

FIG. 2. Fractional ratio of ionization probability as a function of laser intensity. The intensity of the ionizing laser is identical to that of the exciting laser. The schemes of the exciting- and the ionizing-laser bandwidth are shown in the figure.

lowing sections are

$$\Gamma_1 = 2.96I \ , \tag{14}$$

$$\Gamma_{1'} = 2.74I \ , \tag{15}$$

$$\Gamma_{2'} = 3.08I \ , \tag{16}$$

$$\Omega_{01} = 6.18\times 10^7\sqrt{I} \ , \tag{17}$$

$$\Omega_{01'} = -3.57\times 10^7\sqrt{I} \ , \tag{18}$$

$$\Omega_{02'} = -5.05\times 10^7\sqrt{I} \ , \tag{19}$$

which have been obtained by Lambropoulos and Lyras in Ref. [8]. The parameter I denotes a laser intensity whose unit is W/cm^2. We employ a pulse of duration $T_L = 10$ nsec and the profile of the pulse that is linearly increasing during 0.1 T_L, constant to 0.5 T_L, and linearly decreasing to zero [8]. With regard to the laser bandwidth, we adopt 0.04 cm^{-1} [full width at half maximum (FWHM)] as the narrow bandwidth and 0.4 cm^{-1} (FWHM) as the broad bandwidth.

III. RESULTS AND DISCUSSIONS

Figure 2 shows the dependency of β on the intensity for four combinations of the exciting- and ionizing-laser bandwidth. In this figure β is calculated on the condition of identical intensities of the exciting and ionizing lasers. This figure shows that the bandwidth of the ionizing laser does not have an effect on β compared with that of the exciting laser. The bandwidth term plays a role similar to a decay term in the equations. In the scheme studied here, however, the atoms are assumed to be ionized to continuum, which gives rise to no effect on the fractional ratio. Excited with the narrow-bandwidth laser, the even- and odd-mass isotopes are well separated at the intensity between 10^3–10^4 W/cm^2, whereas above 10^5 W/cm^2 the difference of β between the narrow- and broad-excitation lasers becomes very small, which means that the bandwidth of either excitation or ionization has little effect on β at large intensity. Above 10^8 W/cm^2, β is nearly equal to zero because both P and P' approach unity. For the sake of simplicity, we take the broad bandwidth (0.4 cm^{-1}) as the bandwidth of the ionizing laser in the rest of this paper.

To investigate the effect of the exciting-laser bandwidth, we show the time evolution of the population of the even- and the odd-mass isotopes at 10^4 W/cm^2, where the difference of β between the even- and the odd-mass isotopes is apparent. In Fig. 3(a) the exciting-laser bandwidth is so small that population inversion occurs at $T = 1$ nsec, which is a coherent phenomenon. On the other hand, the populations of the even-mass isotopes do not oscillate and saturate to 0.5 in Fig. 3(b). The saturation time of Fig. 3(b) takes more time than that of Fig. 3(a), which means ionization occurs more easily in Fig. 3(a) than in Fig. 3(b). With regard to the odd-mass isotopes, Fig. 3(c) shows that each intermediate level is populated at about 20%, while in Fig. 3(d), $|2'\rangle$ is approximately 40% and $|1'\rangle$ is 30%. The population of $|2'\rangle$ is always larger than that of $|1'\rangle$ because $\Omega_{02'}$ is larger than $\Omega_{01'}$.

We plot the time evolution of the ionization probability of the even- and odd-mass isotopes in Figs. 4(a) and 4(b). These figures show that the ionization probability is of the order of 10^{-4}, which cannot be observed in Fig. 2. With the narrow-bandwidth laser, the even-mass isotopes

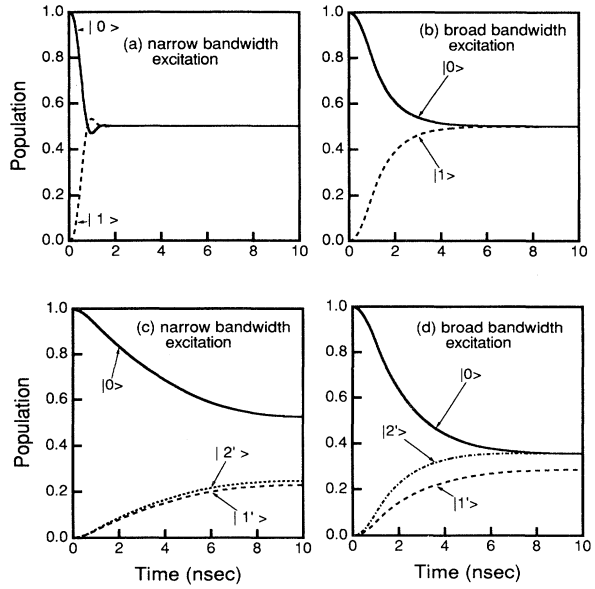

FIG. 3. Time evolution of the populations with the exciting- and ionizing-laser intensity at 10^4 W/cm^2. (a) The population of the even-mass isotopes with the narrow-band laser. (b) The population of the even-mass isotopes with the broadband laser. (c) The population of the odd-mass isotopes with the narrow-band laser. (d) The population of the odd-mass isotopes with the broadband laser. The notations such as $|0\rangle$, $|1\rangle$, $|1'\rangle$, and $|2'\rangle$ are indicated in Fig. 1.

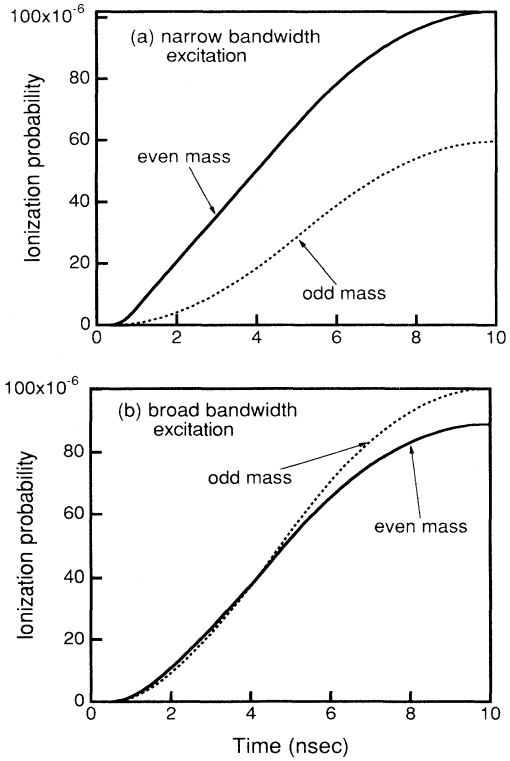

FIG. 4. Time evolution of the ionization probability with the exciting- and ionizing-laser intensity at 10^4 W/cm^2 (a) with the narrow-band laser and (b) with the broadband laser.

are more ionized, as shown in Fig. 4(a), while the ionization probability of the odd-mass isotopes exceeds that of the even-mass isotopes at 4 nsec in Fig. 4(b). The result of Fig. 4(a) implies that the laser configuration can be utilized for laser-isotope separation, while Fig. 4(b) shows that if laser bandwidth is broad enough to overlap all hyperfine structures the odd-mass isotopes would be more ionized than the even-mass isotopes, even though the even-mass isotopes are excited as resonance. The ionization probability of the odd-mass isotopes is greater than that of the even-mass isotopes after 4 nsec, because the total population of the intermediate levels of the odd-mass isotopes is about 60% at the time, while that of the even-mass isotopes is about 50%. This saturation makes the inversion of the ionization probability.

We compare the time evolution of the population of the even- and odd-mass isotopes at 10^8 W/cm^2 where the exciting-laser bandwidth does not make any difference to β. In Fig. 5(a) a more rapid Rabi oscillation is observed than in Fig. 5(b), because of the coherence of the narrow bandwidth. The population difference of the population between the ground level and the intermediate levels of the odd-mass isotopes in Fig. 5(d) is smaller than in Fig. 5(c), because the intermediate levels in Fig. 5(d) are more excited by the broad bandwidth that overlaps them.

We also plot the time evolution of the fractional ratio β at 10^4 W/cm^2 and 10^8 W/cm^2 with the narrow- [Fig. 6(a)] and the broad- [Fig. 6(b)] bandwidth exciting laser. In Fig. 6(a), the even-mass isotopes are selectively ionized at 10^4 W/cm^2, whereas the odd-mass isotopes are more ion-

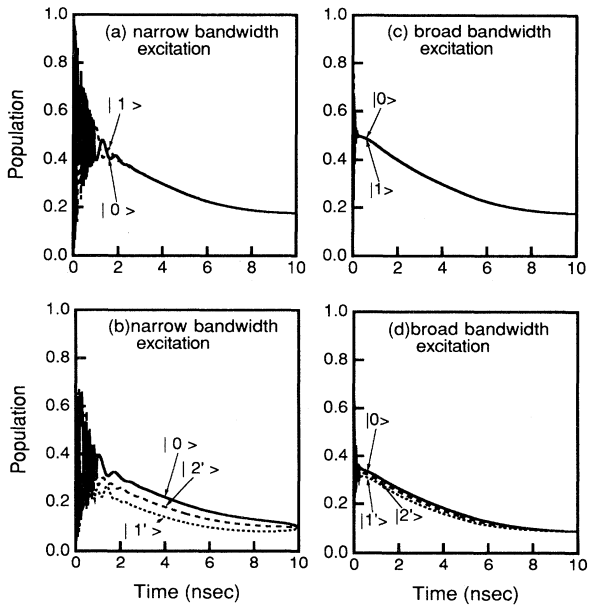

FIG. 5. Time evolution of the population with the exciting- and ionizing laser intensity at 10^8 W/cm^2. (a) The population of the even-mass isotopes with the narrow-band laser. (b) The population of the odd-mass isotopes with the narrow-band laser. (c) The population of the even-mass isotopes with the broadband laser. (d) The population of the odd-mass isotopes with the broadband laser.

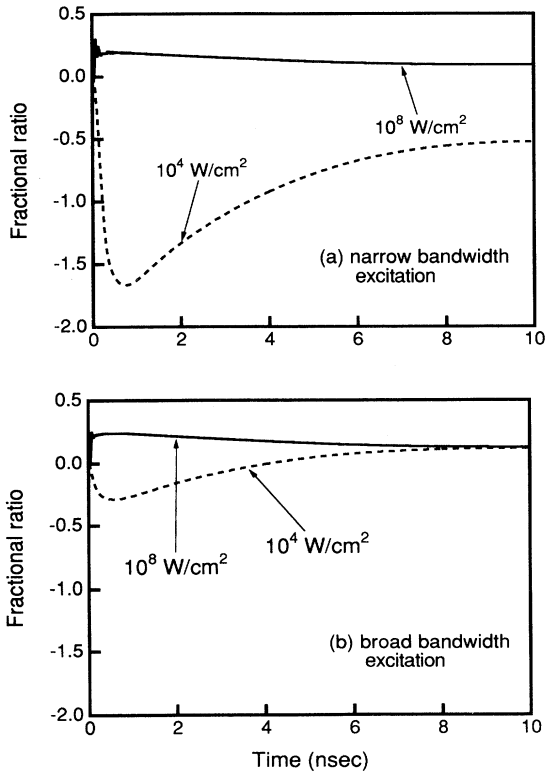

FIG. 6. Time evolution of fractional ratio with the exciting- and ionizing-laser intensity at 10^4 W/cm^2 and 10^8 W/cm^2 (a) with the narrow-band laser and (b) with the broadband laser.

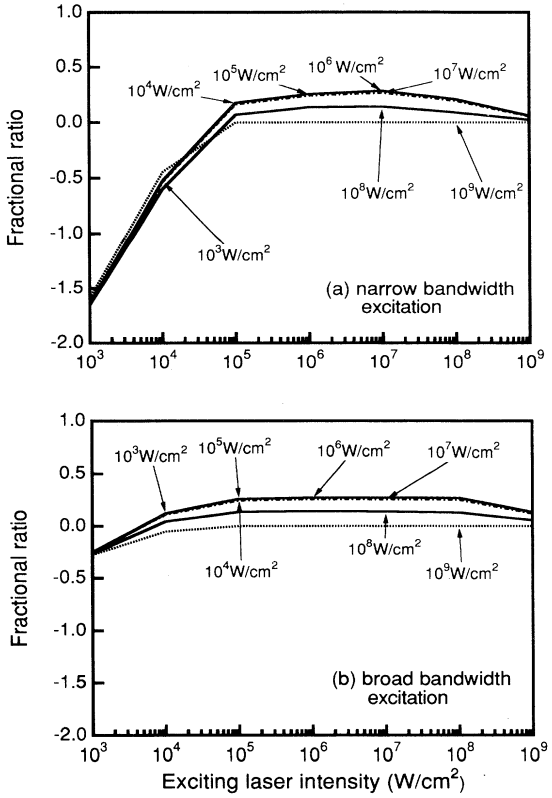

FIG. 7. Fractional ratio as a function of the exciting-laser intensity. The intensity indicated in the figure is the ionizing-laser intensity (a) with the narrow-band laser and (b) with the broadband laser.

ized all times at 10^8 W/cm^2 because of the saturation of all levels. However β increases to above zero even at 10^4 W/cm^2 in Fig 6(b). These figures show that the time dependency of β at 10^8 W/cm^2 is the same with the narrow bandwidth as with the broad one. But at 10^4 W/cm^2 the difference of β between the narrow and the broad bandwidths is apparent. In other words, the pulse form plays an important role on the time evolution of the population. Although the case at 10^8 W/cm^2 has a maximum, that at 10^4 W/cm^2 has a minimum at about the same time.

We show the fractional ratio β as a function of the exciting- and ionizing-laser intensity in Fig. 7(a). This figure shows that there is little dependence on ionizing-laser intensity, although β varies with exciting-laser intensity. With a small intensity of the exciting laser, $\beta < 0$, because the even-mass isotopes are resonant and the intensity that excites the odd isotopes is very small. But as the exciting-laser intensity increases, the fractional ratio cannot ignore the intensity that overlaps the levels of the odd-mass isotopes, especially when the ionizing-laser intensity is small. When the intensity is large, the atoms are ionized as soon as they are excited.

On the other hand, Fig. 7(b) shows that the dependency on the laser intensity is smaller than that of the case excited by the narrow-bandwidth laser. As in Fig. 7(a), the fractional ratio in Fig. 7(b) keeps constant in the range between 10^5 and 10^8 W/cm^2, and decreases rapidly to zero. Figure 7(b) shows that the dependency of the fractional ratio on the ionizing-laser intensity is almost the same in the range between 10^5 and 10^8 W/cm^2 of the exciting-laser intensity.

At the exciting-laser intensity of 10^3 W/cm^2, the fractional ratio is below zero for both narrow and broad bandwidths. This shows that the odd-mass isotopes are not so excited as the even-mass isotopes. Figures 7(a) and 7(b) show that the fractional ratios vary rapidly with the exciting-laser intensity between 10^3 and 10^5 W/cm^2 because the intermediate levels are not saturated.

In Fig. 8 we show the dependency of the exciting-laser wavelength on the fractional ratio at various exciting-laser intensities, with an ionizing-laser intensity of 10^5 W/cm^2. Figure 8(a) shows that between 10^5 and 10^9 W/cm^2 the fractional ratio is not so sensitive to the wavelength of the exciting laser, except that clear resonance of the even- and odd-mass isotopes is observed at the exciting-laser intensity of 10^3 W/cm^2. This figure suggests that the exciting-laser intensity has to be fixed to about 10^3 W/cm^2 in order to separate the even and odd-mass isotopes.

When the bandwidth of the exciting laser is broad [Fig. 8(b)], the resonance is not so clear. It has a little dependence on the wavelength, especially with the exciting-laser intensity of 10^3 W/cm^2.

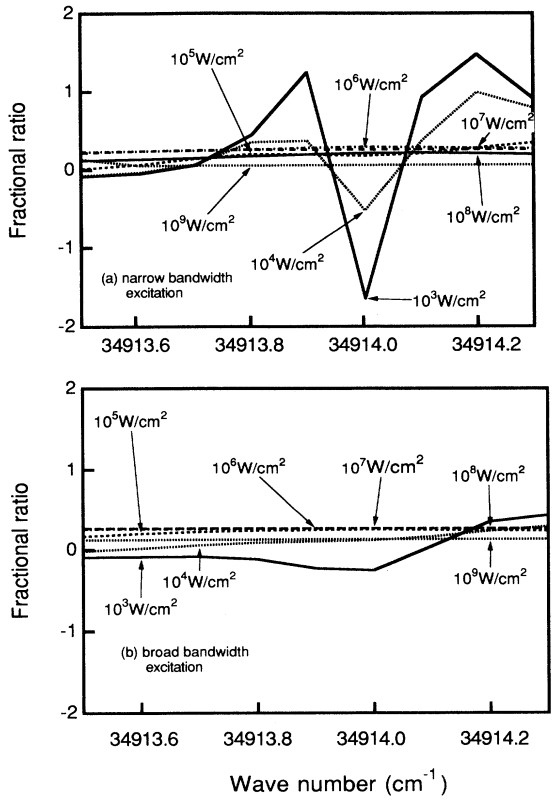

FIG. 8. Fractional ratio as a function of the exciting-laser wavelength. The intensity indicated in the figure is the exciting-laser intensity. The ionizing-laser intensity is 10^5 W/cm^2 (a) with the narrow-band laser and (b) with the broad-band laser.

IV. CONCLUSION

We have investigated the effects of the laser parameters on the fractional ratio of the ionization probability of the even- and odd-mass isotopes of Sn. The fractional ratio β is more dependent on the exciting-laser intensity than on the ionizing-laser intensity. This is because the ionization is the transition from the bound state to the continuum state, but the excitation is from bound state to bound state. When the exciting-laser bandwidth is narrow, only the even-mass isotopes that are on resonance are ionized at the intensity between 10^3–10^4 W/cm^2. This configuration could be utilized for the isotope separation. At the intensity between 10^5–10^6 W/cm^2, the odd-mass isotopes are more ionized than the even ones, because the intensity on the hyperfine levels of the odd-mass isotopes is so large that the hyperfine interaction plays an important role on the laser-atom interaction. As the exciting-laser intensity increases to 10^8 W/cm^2, the fractional ratio β approaches zero because the ionization probabilities of both even- and odd-mass isotopes go to unity. On the other hand, when the exciting-laser bandwidth is large, the odd-mass isotopes are to some degree ionized at even 10^3 W/cm^2. The dependence on the exciting-laser intensity has the same tendency as that with the narrow-bandwidth laser, on condition that the laser intensity is over 10^5 W/cm^2, and the fractional ratio β goes to zero as the intensity increases.

With regard to the exciting-laser wavelength, as the exciting-laser intensity increases, the selectivity decreases, even when the exciting-laser bandwidth is narrow enough to excite only the even-mass isotopes which are on resonance. In this system the even-mass isotopes are ionized approximately equally at the intensity 10^6 W/cm^2 of the narrow-bandwidth laser. However, the fractional ratio is sensitive to the exciting-laser wavelength, even when the exciting-laser bandwidth is broad with the small intensity.

ACKNOWLEDGMENT

The authors would like to thank Dr. J. Ahn for reading the manuscript and making a number of valuable suggestions.

[1] V. S. Letokhov, *Laser Photoionization Spectroscopy* (Academic, New York, 1987).
[2] G. I. Bekov, V. S. Letokhov, and V. N. Radaev, Fresenius, Z. Anal. Chem. **335**, 19 (1989).
[3] C. M. Miller, N. S. Nogar, A. J. Gancarz, and W. R. Shields, Anal. Chem. **54**, 2377 (1982).
[4] D. L. Donohue, D. H. Smith, J. P. Young, H. S. Mckown, and C. A. Pritchad, Anal. Chem. **56**, 379 (1984).
[5] J. D. Fassett, L. J. Powell, and L. J. Moore, Anal. Chem. **56**, 2228 (1984).
[6] R. J. Walker and J. D. Fassett, Anal. Chem. **58**, 2923 (1986),
[7] W. M. Fairbank, Jr., M. T. Spaar, J. E. Parks, and J. M. R. Hutchinson, Phys. Rev. A **40**, 2195 (1989).
[8] P. Lambropoulos and A. Lyras, Phys. Rev. A **40**, 2199 (1989).
[9] A. Lyras, B. Zorman, and P. Lambropoulos, Phys. Rev. A **42**, 543 (1990).
[10] S. Hasegawa, T. Kakudoh, H. Maeda, and A. Suzuki, in *Proceedings of the 18th International Quantum Electronics Conference, Vienna, 1992,* Technical Digest Series (Institut für Nachrichtentechnik der TU Wien, Vienna, 1992), p. 142.
[11] P. Zoller, Phys. Rev. A **20**, 2420 (1979).
[12] A. T. Georges and P. Lambropoulos, Phys. Rev. A **20**, 991 (1979).
[13] P. Zoller, Phys. Rev. A **20**, 1019 (1979).
[14] A. T. Georges, Phys. Rev. A **21**, 2034 (1980).
[15] S. N. Dixit, P. Zoller, and P. Lambropoulos, Phys. Rev. A **21**, 1289 (1980).
[16] A. T. Georges and S. N. Dixit, Phys. Rev. A **23**, 2580 (1981).
[17] P. Zoller, G. Alber, and R. Salvador, Phys. Rev. A **24**, 398 (1981).
[18] P. Zoller, Phys. Rev. A **19**, 1151 (1979).
[19] S. Hasegawa, H. Maeda, T. Kakudoh, and A. Suzuki, Phys. Rev. A **45**, 5065 (1992).
[20] K. Katoh, S. Hasegawa, and A. Suzuki, J. Nucl. Sci. Technol. **27**, 450 (1990).